SCIENTIFIC REPORTS

OPEN

SUBJECT AREAS:
NANOSTRUCTURES
BIOINSPIRED MATERIALS
BIOMEDICAL ENGINEERING
MOLECULAR SELF-ASSEMBLY

Received
15 May 2013

Accepted
27 September 2013

Published
22 October 2013

Correspondence and requests for materials should be addressed to L.F.C. (Chi@uni-muenster.de) or Y.K.L. (yklai@suda.edu.cn)

Bioinspired TiO_2 Nanostructure Films with Special Wettability and Adhesion for Droplets Manipulation and Patterning

Yue-Kun Lai[1,2], Yu-Xin Tang[3], Jian-Ying Huang[2], Fei Pan[1], Zhong Chen[3], Ke-Qin Zhang[2], Harald Fuchs[1] & Li-Feng Chi[1,4]

[1]Physikalisches Institute and Center for Nanotechnology (CeNTech), Westfälische Wilhelms-Universität Münster, Münster D-48149, Germany, [2]National Engineering Laboratory of Modern Silk, and College of Textile and Clothing Engineering, Soochow University, Suzhou 215123, PR China, [3]School of Materials Science and Engineering, Nanyang Technological University, 50 Nanyang Avenue, Singapore 639798, Singapore, [4]Institute of Functional Nano & Soft Materials (FUNSOM), Soochow University, Suzhou 215123, PR China.

Patterned surfaces with special wettability and adhesion (sliding, sticky or patterned superoleophobic surface) can be found on many living creatures. They offer a versatile platform for microfluidic management and other biological functions. Inspired by their precise arrangement of structure and chemical component, we described a facile one-step approach to construct large scale pinecone-like anatase TiO_2 particles (ATP) film. The as-prepared ATP film exhibits excellent superamphiphilic property in air, changes to underwater superoleophobicity with good dynamical stability. In addition, erasable and rewritable patterned superamphiphobic ATP films or three-dimensional (3D) Janus surfaces were constructed for a versatile platform for microfluidic management and biomedical applications. In a proof-of-concept study, robust super-antiwetting feet for artificial anti-oil strider at the oil/water interface, novel superamphiphobic surface for repeatable oil/water separation, and multifunctional patterned superamphiphobic ATP template for cell, fluorecent probe and inorganic nanoparticles site-selective immobilization were demonstrated.

Nature contains amazing surface hierarchical structures and chemical component distribution, which provides bioinspired solutions for solving many of mankind's greatest challenges[1–4]. There are three typical super-antiwetting cases in nature, which are "sliding" superhydrophobic lotus leaves with ultra-low water sliding resistance, superoleophobic shark skin with low oil adhesion underwater, and patterned super-hydrophobic beetle's back with highly hydrophilic/phobic regions[5–7]. Bioinspired surfaces with extreme wetting property (superamphiphobicity/superamphiphilicity) with both water and oil contact angle (CA) above 150° or below 5° respectively, have generated extensive interest during recent years because of their fundamental science and potential industrial applications, such as self-cleaning[8–11], droplet manipulation[12–14], patterning template[15,16], anti-bioadhesion[17,18], and fluidic devices[19,20]. For many of these applications, uniform surfaces with combined special water/oil wettability/adhesion in air or underwater environment, or binary patterned surfaces with high or even ultra-high (above 150°) wetting contrast are required for precise and reliable manipulation of expensive biofluids and droplets. Compared to vast reports of uniform superhydrophobic or superhydrophilic surfaces for high surface tension droplet under atmosphere environment, few studies reported the patterned superoleophobic surfaces, Janus super-antiwetting interfaces, and reversible superamphiphobic surfaces in air or underwater conditions. Recently, several attempts have been developed to fabricate such special super-antiwetting surface, for example, Tuteja and co-workers reported a facile methodology to create a patterned superamphiphobic surface by electrospinning polymer solution followed by selective O_2 plasma treatment. They used this patterned superamphiphobic surfaces as confining templates for wettability-driven site-specific self-assembly of micro-particles and polymers[21]. Xue *et al.* reported a temperature controlled water/oil wettability of a surface constructed by a block copolymer (BCP) surface, which exhibited a dual water/oil on-off switch for selective permeation through the BCP-coated mesh[22].

Specific anatase TiO_2 nanostructures have become a focus of tremendous interests due to their good biocompatibility and excellent photocatalytic activity to change surface chemical composition[23–25]. Therefore, the resultant wettability on TiO_2 surface can be greatly influenced by UV irradiating and amplified by roughness of nanostructures. In this work, we applied a simple one-step and practical electrochemical anodizing approach to

fabricate large scale pinecone-like anatase TiO_2 particles (ATP) film. The as-prepared environment-responsive ATP film exhibits superamphiphilic property in air, and changes to excellent superoleophobicity underwater. The combined superamphiphobicity in air and superoleophilicity underwater with good dynamic stability can be achieved by a hydrogen-bond-driven process for *1H, 1H, 2H, 2H*-perfluorodecyltriethoxysilane (PFDS) assembling. In addition, erasable and rewritable patterned superamphiphobic ATP film with extreme wettability contrast (superamphiphilic/superamphiphobic) or three-dimensional (3D) unsysmmetric Janus surface can be constructed by alternating photocatalytic lithography and monolayer self-assembly. The 3D functional surface with superwetting/antiwetting properties would be a versatile platform in a wide range of applications, especial for microfluidic management (e.g., microdroplets manipulator, anti-biofouling, microreactor, and oil/water separation) and biomedical applications. In a proof-of-concept study, we investigated oil/water separation of the superamphiphobic surface underwater, and cell site-selective immobilization using the 3D patterned superamphiphobic ATP film. The patterned superamphiphobic ATP surface can serve for multi-functional applications including bioactive scaffolds for site-selective cell immobilization and high contrast wettability templates for metal nanoparticles assembling.

Results

Figure 1a, b show the typical top and cross-sectional SEM images of the as-anodized anatase TiO_2 particles (ATP) film, respectively. It is seen that the surface has uniformly-distributed pinecone-like ATP protrusions with radial multilayer nanoflakes grew out on Ti substrate to form fractal structure, the bottom diameter and height of the vertically orientated pinecone-like ATP protrusions is approximately 1.0–4.0 μm and 0.5–5.0 μm, respectively. Figure 1c shows the low magnification TEM images of the micro-size ATP structure. The hierarchical pinecone-like structure has the rough surface, which is composed of numerous plate-like nanosheets (inset of 1c). From the high-resolution TEM image in Figure 1d, it is observed that the plate-like sheets is composed of polycrystalline anatase based on the observation of the different plane of anatase phase and the appearance of the moiré fringes (ellipse circle). This result is also verified by the XRD result in Figure 1f. Four broad diffraction peaks at 2θ = 25.4, 37.8, 48.0, 54.5° can be assigned to anatase TiO_2 of (101), (004), (200), and (105) planes, respectively (JCPDS No. 21-1272). The current work proves that crystalline anatase TiO_2 can be directly fabricated by a facile one-step electrochemical anodizing process in an environmentally-friendly electrolyte without the assistance of annealing process. During experiment, it was observed that the electrolyte temperature increased to 40–60 °C by 50 V anodizing for 4 h due to the local exothermic heat caused by the vigorous electrochemical process. The increased electrolyte temperature provides a greater driving force for ionic conduction and enhances the crystalline phase formation. Moreover, the surface of the ATPs becomes rougher as the electrochemical anodization process prolongs. Therefore, we attribute the crystallization of the amorphous TiO_2 nanostructures to the dissolution and recrystallization mechanism. Similar results on the special role of the water in the transformation from amorphous TiO_2 to anatase TiO_2 at low temperature were also reported[26,27], which only occurred during the sol-gel processes. This is different from conventional TiO_2 nanotube arrays anodization in harmful HF solution, where the as formed TiO_2 is amorphous. Alternatively, protonated titanate nanostructures can be obtained by anodization in high concentration electrolyte under a high anodizing voltage, they have to be heated to above 300 °C to form crystalline anatase[28–30].

Water or oil rapidly spreads and wets the as-prepared ATP film in air due to high surface energy of the hydroxylated surfaces verified by FTIR characterization (Figure S1, SI), indicating the superamphiphilicity of the sample. To our surprise, such superamphiphilic surfaces are also oil-repellent when placed underwater because the surface is pre-coated with a thin layer of water that could not be penetrated by oil (Figure 1e and Movie S1, SI). Even more, similar to the oil droplet on the underwater superoleophobic materials, air bubbles are repelled from the submerged surface to retain a nearly spherical shape and are able to move around freely, exhibiting an underwater superaerophobic behavior coupled with low adhesion. Such excellent

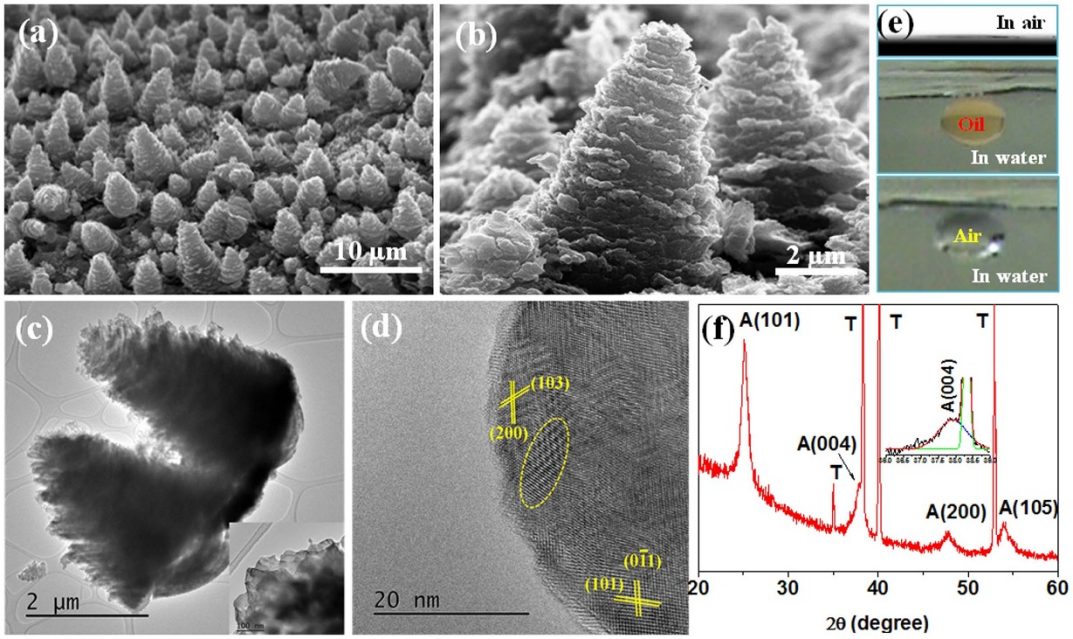

Figure 1 | Typical top and cross-sectional SEM (a,b) and TEM (c,d) images of the as-anodized hierarchical pinecone-like structure ATP film. The inset of 1c shows the top-view TEM image of a single ATP. (e) Optical image of the water droplet in air (top), underwater oil droplet (middle) and air bubble (bottom) on the as-prepared superamphiphilic ATP surface. (f) XRD pattern of the as-prepared ATP film. The inset of 1f shows the enlarge peak of A (004). A and T represents anatase TiO_2 and titanium substrate, respectively.

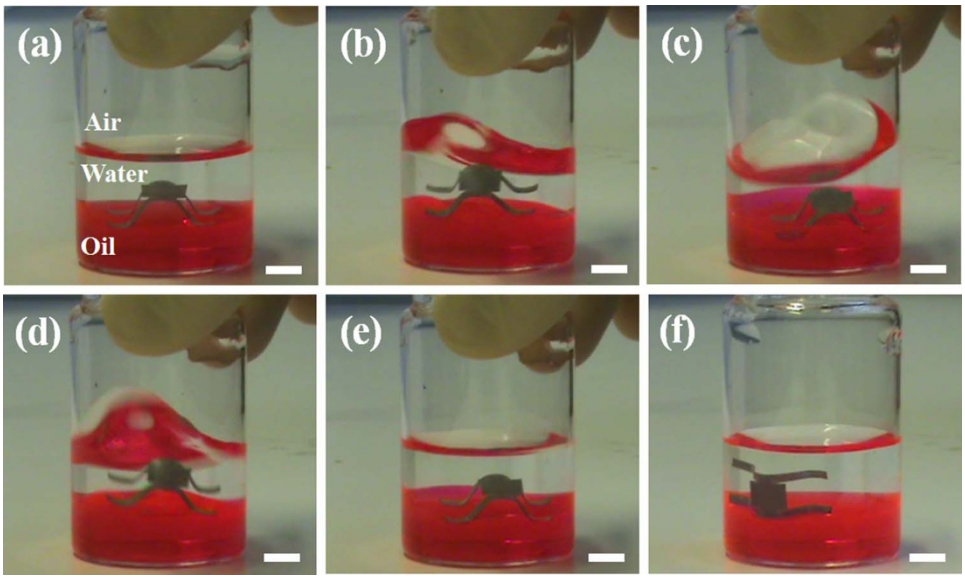

Figure 2 | **The dynamic stability of the anti-oil strider's floating at the oil/water interface.** The scale bar is 5 mm.

underwater superamphiphobic (superoleophobic & superaerophobic) surface with good dynamic stability could provide a versatile platform in a wide range of applications, especial for microfluidic devices, e.g., oil droplet manipulation and transportation tools, underwater micro-reactors, and gas bubbles collectors[31–34].

In a proof-of-concept study, we constructed an artificial anti-oil strider with four underwater super-antiwetting feet (**Figure 2**). The legs of the artificial anti-oil strider are as-prepared ATP coated Ti plates. To distinguish the oil/water interface, the oil (1,2-dichoroethane) is dyed red. When the anti-oil strider is put on the water surface, it immediately sinks down and finally resides at the oil/water interface. Obvious crescent-shaped meniscuses are generated around the legs. Supported by the huge curvature force and buoyancy force, the artificial oil strider can stand easily at the interface (Figure 2a). The stability of the oil strider floating at the oil/water interface was also tested in our experiment (Movie S2, SI). As the interface strongly waves, the oil strider moves up and down but never sinks into the oil layer below (Figure 2b–e). Even when turned aside, the oil strider still stably stood on the oil surface due to the huge superoleophobic force (Figure 2f). When the oil strider was taken out from the oil/water system, no oil residue was adhered on its legs. These results further indicate that the artificial legs have excellent dynamic superoleophobicity in water.

Furthermore, we built an underwater superoleophobic system consisting of a pair of oil-repellent tweezers utilizing the superoleophobic ATP plates. Through manipulating the tweezer tips, the oil droplet could be captured, lifted and transported to another superoleophobic substrate without any loss (Figure S2, and Movie S3, SI). If released to a superoleophilic surface, the oil droplet will be dispersed on the surface, achieving on-demand manipulation of oil droplets in water. By controlling the wettability of the ATP surface, we can also realize a topographically regulated wettability and adhesion on superoleophobic ATP surfaces underwater by adjusting the anodizing time to control the size and density of microscale protrusions. Oil droplets could be rapidly transported to targeted places by utilizing of the high adhesion contrast (Figure S3, and Movie S4, SI).

FESEM analysis of the effect of deposition time on the surface morphologies indicates that the film structure is consistent with an instantaneous two dimensional (2D) to 3D growth mechanism (**Figure 3**). Initially, a smooth thin layer of nanoparticles with sparsely out-growth of flower-like microparticles was formed on the titanium substrate (Figure 3a–c and f). Subsequently, the microparticles

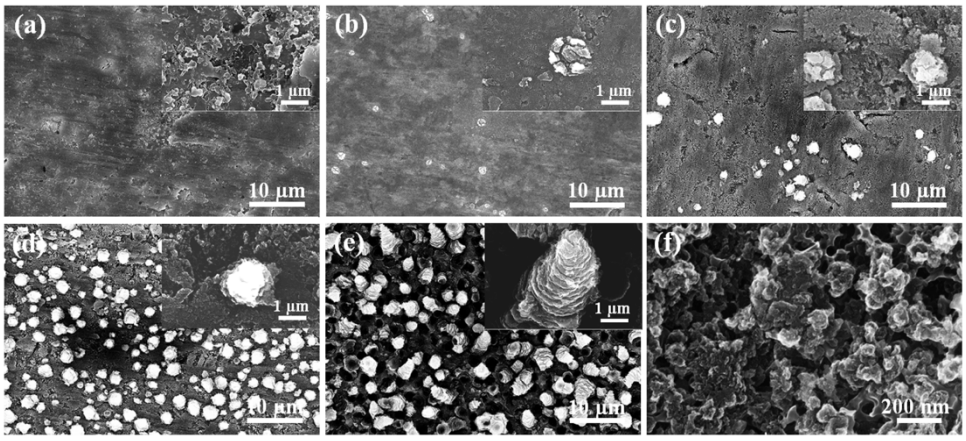

Figure 3 | FESEM images of ATP films by electrochemical anodizing in 0.01 M NH_4F solution on titanium substrates at 50 V for (a) 2 min; (a) 10 min; (c) 30 min; (d) 60 min; (e) 240 min. (f) Magnified image of 3c. The insets show the corresponding magnified image of nanoparticles layer.

gradually grew along the vertical direction of the substrate with the new nanoflakes formed at the bottom, forming a pinecone-like forest film (Figure 1a in the main text). With longer anodizing time, part of the microparticles were detached from the substrate leaving a concave hole to form 3D rough ATP film (Figure 3e).

Except the influence of surface morphology and the film roughness, the anodizing time also have a great effect on the oil (1,2-dichloroethane) wettability and adhesion in air or underwater. Although all the as-prepared surfaces have the similar high hydrophilicity or even supehydrophilicity in air, the oil contact angle and dynamic properties are rather different underwater. When the reaction time was less than 5 min, oil droplet cannot roll off the underwater surface (**Figure 4**a). Increasing the reaction time to 5 min, the contact angle increases to 157° but the oil droplet still firmly adhered on the superoleophobic substrate even when the sample is tilted vertically (90°). Further increasing the reaction time, the contact angle increases slowly to a platform, but the sliding angle sharply decrease to below 4° exhibiting a superoleophobic state with ultralow oil adhesion underwater. These results indicate that we can construct both low- and high-adhesion superoleophobic surface underwater with mimicking lotus and petal effects. After PFDS modification with a hydrogen-bond-driven process, the as-prepared hydrophilic or superhydrophilic surfaces turn to superamphiphobicity in air. The change of contact angle and oil adhesion followed the similar trend as that of the as-prepared samples underwater (Figure 4b). However, these superamphiphobic samples in air display contrary superoleophicity underwater with a good reversibility owing to the trapped air layer at the solid-liquid interface. We also envisage that such special surface with superamphiphobic properties in air and superoleophilic/aerophilic property underwater would be a low cost platform for effective underwater oil or air capture.

When the as-prepared hydroxylated ATP surface is modified by *1H, 1H, 2H, 2H*-perfluorodecyltriethoxysilane (PFDS) by a hydrogen-bond-driven process (**Figure 5**a), the outer terminated hydroxyl groups (-OH) change to low surface energy fluorocarbon groups (-CF_x). This result is verified by XPS measurement (Figure S4, SI). Water and oil CA (n-hexadecane, 27.5 mN m^{-1}) on the film in air is about 164° and 155° (Figure 5b), respectively showing the good superamphiphobic character in air. Moreover, the unstable spherical droplets moved easily on this surface and rolled off with a tilting angle lower than 5° due to the ultra-low adhesion of the solid-liquid interface. This is ascribed to the fluorocarbon group that provides a low energy surface, as well as a thin layer of air trapped in the rough 3D hierarchical pinecone-like ATP. This type of structure contributes greatly to the amphiphobicity increase and results in the super-antiwetting performance for water and oil[35,36]. However, when placed in water, the oil and bubble wettability varied so drastically that oil droplets and air bubbles spread out quickly once in contact with the water submerged PFDS-derived surface (Figure 5b). The contact angle of oil and bubble under water is about 0°, showing superoleophilic and superareophilic property. In order to evaluate the repeatability, the surfaces were placed in air and in water repeatedly for several times. The wettability could be reversibly changed between being superamphiphobic in air and superoleophilic in water for many cycles (Figure 5c).

The 3D functional surface patterns would be a versatile platform in a wide range of applications, e.g., friction reduction, self-cleaning, and water/oil separation. In a proof-of-concept study, we applied the PFDS-modified pinecone-like ATP plates (superoleophobic in air and superoleophilic underwater) as "oil capture hands" to gather oil droplets in water (Figure 5d and Movie S5, SI). We first placed a layer of oil droplets (1,2-dichloroethane) under water in a glass container (process 1). Then a PFDS-modified ATP plate was used to capture the oil drops underwater (process 2). Under the collection force, the oil droplets coalesce on the plate surface. When the plate was lifted out of the water, the captured oil droplets accumulated into one large volume (process 3). More importantly, it is worth noting that the plate kept self-cleaning without any oil residue due to the excellent superamphiphobic property in air. This is different from the conventional superhydrophobic surface that is completely oil contaminated after oil absorption in water, which makes it difficult for repeated use. The collected oil was then extracted from the water surface easily to achieve effective water/oil separation (process 4–6). This study opens up a new strategy for the treatment of oily waste water, which has a significant potential for future industrial applications[37–39].

Figure 6a shows the superamphiphobic/superamphiphilic Janus interface materials floating on the water by controlling the surface chemical components with UV irradiation. The upper PFDS modified ATP side shows superoleophobicity with an oil (n-hexadecane) contact angle of 155.0 ± 1.5° in air, while the lower side irradiated by UV light exhibits air superamphiphilicity and underwater superoleophobicity with oil contact angle of 171.5 ± 1.0° in water. The upper side of ATP surface, which acts as an artificial lotus leaf, is only partly wetted by water or oil. The larger amount of trapped air results in superamphiphobicity (Figure 6b). The lower side, which mimics the shark skin, is completely wetted with a thin layer of water (illustrated in light blue color). The micro/nano-structure and trapped water layer greatly reduces the contact area between oil (yellow) and the surface, which achieves underwater superoleophobicity. By this tactics we can simultaneously achieve superamphiphobicity in air and underwater environments by constructing the 3D unsysmmetric wettability interfaces. On the contrary, it becomes superamphiphilic if we reverse the Janus substrate on water surface.

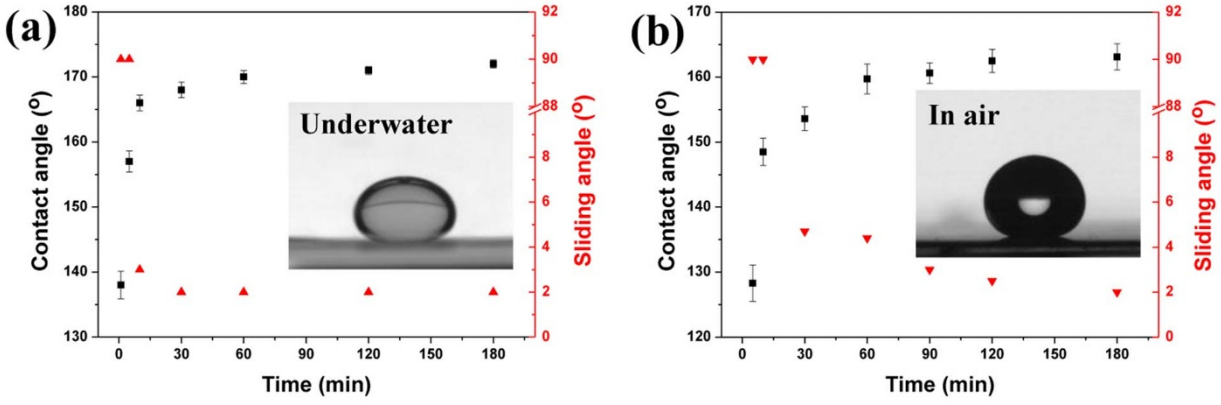

Figure 4 | The correlation between oil contact angle and sliding angle with the electrochemical anodizing time of the as-prepared ATP surface underwater (a) and PFDS modified ATP surface in air (b). The inset of (a) and (b) shows the oil droplet on the as-prepared ATP surface (3 h) underwater and PFDS modified ATP surface in air, respectively.

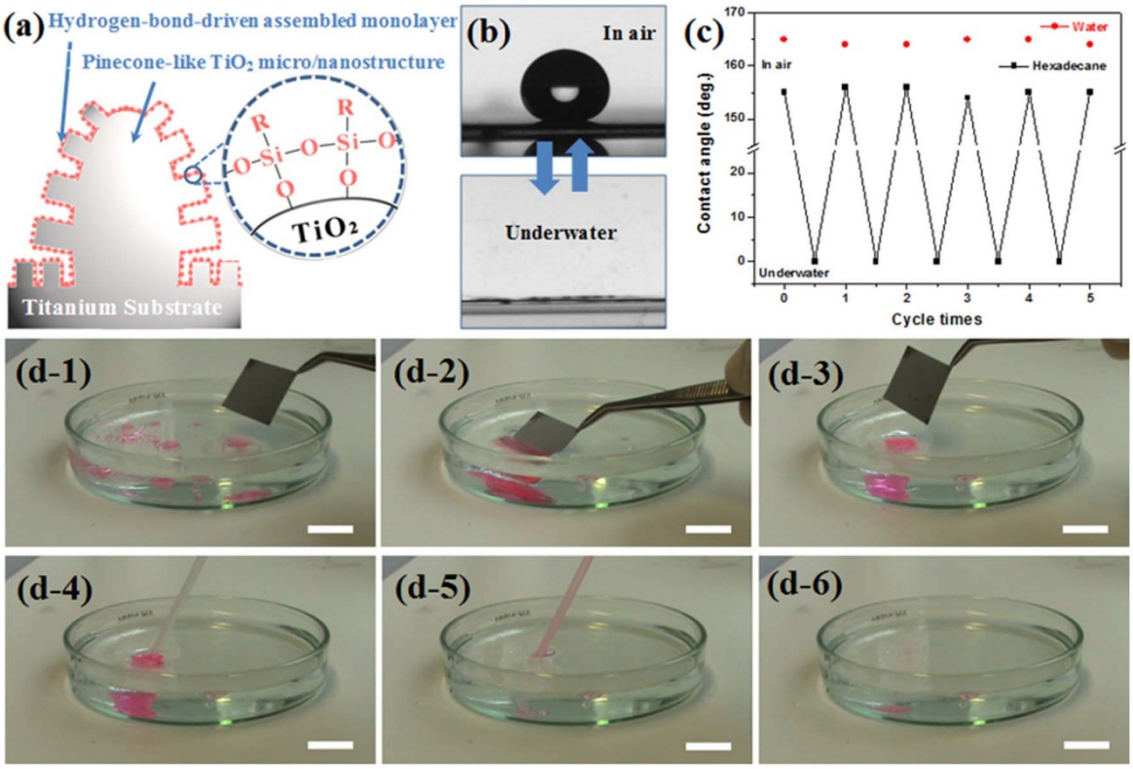

Figure 5 | (a) The PFDS surface modification with a hydrogen-bonding-driven self-assembled process on the hydroxylated ATP surface. (b) The oil droplet image on the PFDS modified ATP surface in air or underwater environment. (c) The reversible wettability change of oil droplet on the ATP surface by alternating the environment. (d) The oil capture and collection process with a superoleophobic plate and underwater superoleophilic property. Process 1–2: a superoleophobic plate touches and captures the underwater oil drops sprayed in bottom of a glass container. Process 3: the captured oil drops gathered together underwater as the superoleophobic plate moves out. Process 4–6: the gathered oil droplets are collected from the water. The oil was colored pink for convenient observation through the capture and collection process.

Compared with the single anti-wetting performance of lotus leaf and shark skin in air and water respectively, such artificial novel Janus interface materials combine the superamphiphobic property of lotus leaf and superoleophobic property of shark skin: they exhibit higher oil contact angle and good chemicals stability in water with an identical micro/nano-structure. Moreover, by controlling the site-selective exposure of UV light with desired geometry, patterned superoleophilic or even patterned superamphiphilic surfaces with fine resolution can be easily constructed by taking advantage of the excellent photocatalytic activity of anatase TiO_2 to decompose the PFDS layer. When such a patterned surface is dipped in hexadecane (dyed yellow), hexadecane selectively wets the superamphiphilic domains, resulting in the well-controlled self-assembly of hexadecane droplets within the superamphiphilic patterns (Figure 6d, and Movie S6, SI). Similar self-assembly of hexadecane droplets with clear boundaries is also achieved by dropping hexadecane on the patterned superamphiphobic surface ascribed to its low contact angle hysteresis. Furthermore, the patterned superamphiphobic surfaces can be reversibly erased and re-generated (Figure S5). Such self-assembled organic liquids arrays can serve as surface-directed microchannels and microreactor arrays for liquid-phase reactions.

Titania is known to possess good biocompatibility, superior mechanical properties, and excellent corrosion resistance. The patterned superamphiphobic ATP substrates can act as potential 3D bioactive scaffolds for site-selective cell immobilization. **Figure 7**a, b show the 3T3 cells on superamphiphobic ATP surface with different wettability patterns in a large area by a general cell media immersion process. 3T3 cells were found to preferentially immobilize on the superamphiphilic regions to form well-defined cell patterning (Figure 7c). They adhered with high affinity to both the top and lateral surface of the ATPs, and good cellular adhesion with extracellular matrix extensions between adjacent ATPs on the superamphiphilic regions (Figure 7d) would provide an excellent support for the survival of cultured cells on biocompatible substrates. On the contrary, cells were seldom found attached to the superamphiphobic regions. The microscale protrusions of ATP are beneficial for cell attachment and activation. Such simple photoresist-free patterning technique using conventional UV light (366 nm) to quickly create various micropatterns on biocompatible superamphiphobic ATP substrate in a large scale provides a potential solution for highly selective cell immobilization and patterning. In addition to the 3D bioactive scaffolds for site-selective cell immobilization, such high contrast wettability template can also be used to construct various well-defined surface patterns, such as drug and biomolecule probes (Figure S6, SI), copper nanoparticles (Figure S7, SI) in a highly selective manner. The 3D functional surface patterns would be a versatile platform in a wide range of applications, especial for biomedical devices (e.g., high-throughput molecular sensing, targeted antibacterial and drug delivery)[40–42].

Discussion

In summary, we have successfully created ATP surface with special wettability in air or underwater environment, and patterned superamphiphobic ATP surface and novel Janus surface with high wettability and adhesion contrast through the photocatalytic degradation of organic layer. The wettability patterns and Janus interfaces on ATP samples can be quickly removed and regenerated by a combination of UV illumination and self-assembly, and adhesion on superamphiphobic ATP surface can also be reversibly regulated between sticky and sliding by controlling the size and density of ATP.

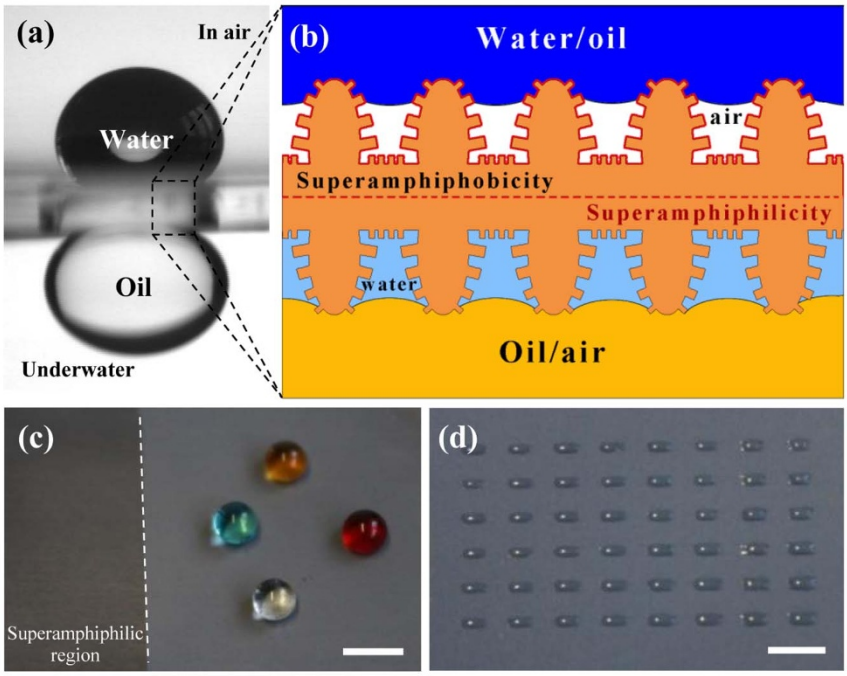

Figure 6 | (a) Digital photographs of a novel ATP sample with Janus interfaces (in air: superamphiphobic upper side and superamphiphilic lower side) floating on the water surface showing the superamphiphobic behavior for water, oil droplets, and air bubbles underwater in air or water environment. Water (dyed blue) and oil (n-hexadecane dyed yellow) droplets form spheres on the superamphiphobic upper side. The oil droplets stay as perfect spheres in water on its lower side. (b) Schematic illustrations of liquid droplets/air bubbles in contact with the identical structured surface with Janus interface wettability. (c) PFDS modified pinecone-like ATP surface that was exposed to UV light on the left (superamphiphilic) and un-illuminated area on the right (superamphiphobic). Water completely wets the superamphiphilic region, but shows a high contact angle of hexadecane (dyed yellow), rapeseed oil (white), ethylene glycol (dyed red), and water (dyed blue) on the superamphiphobic region. (d) Site-selective self-assembly of hexadecane droplets within the superamphiphilic arrays after dipping in hexadecane. The scale bar is 5 mm.

Moreover, applications of patterned superamphiphobic ATP surface in water, oil self-assembly and site-selective cell immobilization were also demonstrated. The results provide new insights into how to control the wettability and adhesion on ATP surfaces by adjusting the topographical structure and surface chemistry. This simple one-step, environmental-friendly and reversible patterning technique with a rapid, precise wetting and adhesion switching can be further extended to a variety of superhydrophobic functional substrates for a number of applications including microdroplets manipulation, water/oil separation, microcontainer and template, and lab-on-a-chip devices.

Methods

Preparation and modification of ATP films. Titanium sheets (purity 99.7%), ammonium fluoride (NH_4F) and 1H, 1H, 2H, 2H-perfluorodecyltriethoxysilane (PFDS) were purchased from Sigma-Aldrich (Germany). The hierarchical ATP films

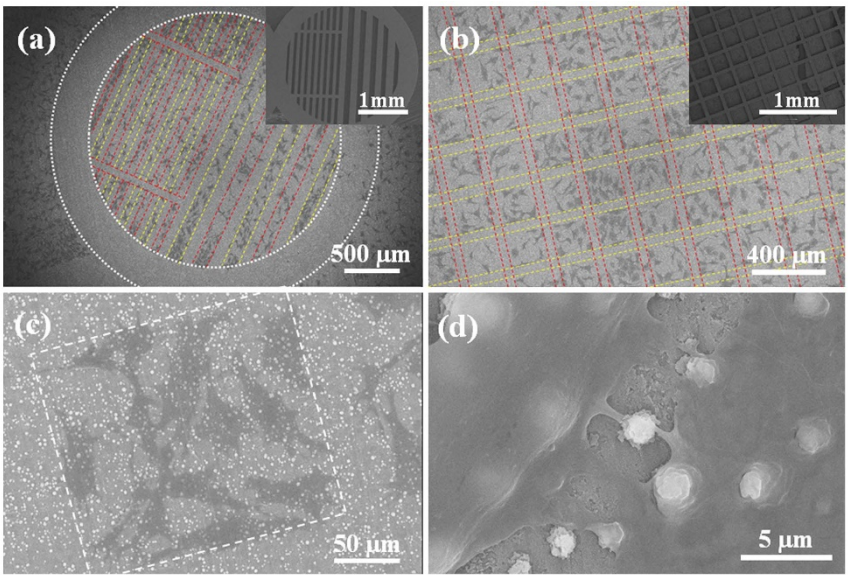

Figure 7 | (a, b) SEM images of 3T3 cells cultured on patterned superamphiphobic ATP surface by a general media immersion process for 24 h. (c, d) High magnified image of (b). The inset of (a, b) shows the corresponding mask for the patterning.

were fabricated by electrochemically anodizing of titanium sheets in 0.01 M NH_4F electrolyte with Pt counter electrode. The anodizing process was carried out at 50 V for a certain time. The ATP film was rinsed with deionized water, dried and immersed in a mixed methanolic solution of hydrolyzed 1 v% of PFDS for 1 h to chemically bind monomolecular layer by a hydrogen-driven process, and baked at 140°C for 1 h.

Characterization of ATP films. The morphology and structure of the ATP nanostructure film was examined by a field-emission scanning electron microscope (FESEM, JEOL JSM-6700F) and transmission electron microscope (TEM, JEOL JEM-2100F). The crystallinity of the samples before and after annealing treatment was measured using an X-ray diffractometer with Cu K_α radiation (XRD, Phillips X'pert-PRO PW3040). The chemical compositions were studied by X-ray photoelectron spectroscopy (XPS, VG ESCALAB MK II) using a 300 W Al Kα X-ray source (1486.6 eV photons) with a base pressure about 3×10^{-9} mbar. The static contact angles and sliding angles were measured at ambient temperature using an OCA 20 instrument (Dataphysics, Germany). Drops of four microliters of various probe liquids were used, and the values reported were the average of five drops per sample at different locations.

Cell culture. 3T3 cells (Mouse embryonic fibroblast cell line) were cultured in Dulbecco's Modified Eagle Medium (DMEM, PAA Laboratories, Pasching, Austria) supplemented with 10% fetal bovine serum (FBS, Invitrogen) under standard cell culture conditions (37°C, 5% CO_2). Cells were detached from the culture dishes by trypsin/EDTA (0.25% trypsin/1 mM ethylenediaminotetracetic acid) solution followed by centrifugation (1200 rpm, 4 min). The pellet was re-suspended in fresh medium. Before the cell seeding, the substrates were washed by 70% ethanol and phosphate buffered solution (PBS). The initial cell seeding number was 1×10^5 cells/cm^2. For the optical microscopy analysis, cells were initially fixed with 2% paraformaldehyde (PFA), 2% glutaraldehyde (GA) in 0.1 M cacodylate buffer (pH 7.4), and dehydrated in a graded series of ethanol.

1. Feng, L. *et al.* Super-hydrophobic surfaces: from natural to artificial. *Adv. Mater.* **14**, 1857–1860 (2002).
2. Liu, K. S. & Jiang, L. Multifunctional Integration: From Biological to Bio-Inspired Materials. *ACS Nano* **5**, 6786–6790 (2011).
3. Zheng, Y. M. *et al.* Directional water collection on wetted spider silk. *Nature* **463**, 640–643 (2010).
4. Deng, X., Mammen, L., Butt, H. J. & Vollmer, D. Candle soot as a template for a transparent robust superamphiphobic coating. *Science* **335**, 67–70 (2012).
5. Barthlott, W. & Neinhuis, C. Purity of the sacred lotus, or escape from contamination in biological surfaces. *Planta* **202**, 1–8 (1997).
6. Liu, M. J., Wang, S. T., Wei, Z. X., Song, Y. L. & Jiang, L. Bioinspired design of a superoleophobic and low adhesive water/solid interface. *Adv. Mater.* **21**, 665–669 (2009).
7. Parker, A. R. & Lawrence, C. R. Water capture by a desert beetle. *Nature* **414**, 33–34 (2001).
8. Nakajima, A. *et al.* Transparent superhydrophobic thin films with self-cleaning properties. *Langmuir* **16**, 7044–7047 (2000).
9. Furstner, R., Barthlott, W., Neinhuis, C. & Walzel, P. Wetting and self-cleaning properties of artificial superhydrophobic surfaces. *Langmuir* **21**, 956–961 (2005).
10. Bhushan, B. & Joch, Y. C. Self-cleaning efficiency of artificial superhydrophobic surfaces. *Langmuir* **25**, 3240–3248 (2009).
11. Lai, Y. K. *et al.* Transparent superhydrophobic/superhydrophilic TiO_2-based coatings for self-cleaning and anti-fogging. *J. Mater. Chem.* **22**, 7420–7426 (2012).
12. Nakajima, A. Design of hydrophobic surfaces for liquid droplet control. *NPG Asia Mat.* **3**, 49–56 (2011).
13. Liu, X. J., Liang, Y. M., Zhou, F. & Liu, W. M. Extreme wettability and tunable adhesion: biomimicking beyond nature? *Soft Matter* **8**, 2070–2086 (2012).
14. Liu, M. J. *et al.* Reversible underwater switching between superoleophobicity and superoleophilicity on conducting polymer nanotube arrays. *Soft Matter* **7**, 4163–4165 (2011).
15. Lai, Y. K., Pan, F., Xu, C., Fuchs, H. & Chi, L. F. In situ surface-modification-induced superhydrophobic patterns with reversible wettability and adhesion. *Adv. Mater.* **25**, 1682–1686 (2013).
16. Ueda, E. & Levkin, P. A. Emerging applications of superhydrophilic-superhydrophobic micropatterns. *Adv. Mater.* **25**, 1234–1247 (2013).
17. Geyer, F. L., Ueda, E., Liebel, U., Grau, N. & Levkin, P. A. Superhydrophobic-superhydrophilic micropatterning: towards genome-on-a-chip cell microarrays. *Angew. Chem. Int. Edit.* **50**, 8424–8427 (2011).
18. Neto, A. I., Custodio, C. A., Song, W. L. & Mano, J. F. High-throughput evaluation of interactions between biomaterials, proteins and cells using patterned superhydrophobic substrates. *Soft Matter* **7**, 4147–4151 (2011).
19. Su, B., Wang, S. T., Song, Y. L. & Jiang, L. Utilizing superhydrophilic materials to manipulate oil droplets arbitrarily in water. *Soft Matter* **7**, 5144–5149 (2011).
20. Liu, X. L. *et al.* Bioinspired oil strider floating at the oil/water interface supported by huge superoleophobic force. *ACS Nano* **6**, 5614–5620 (2012).
21. Kobaku, S. P. R., Kota, A. K., Lee, D. H., Mabry, J. M. & Tuteja, A. Patterned superomniphobic-superomniphilic surfaces: templates for site-selective self-assembly. *Angew. Chem. Int. Ed.* **51**, 10109–10113 (2012).
22. Xue, B. L., Gao, L. C., Hou, Y. P., Liu, Z. W. & Jiang, L. Temperature controlled water/oil wettability of a surface fabricated by a block copolymer: application as a dual water/oil on–off switch. *Adv. Mater.* **25**, 273–277 (2013).
23. Fujishima, A., Zhang, X. T. & Tryk, D. A. TiO_2 photocatalysis and the related surface phenomena. *Surf. Sci. Rep.* **63**, 515–582 (2008).
24. Paramasivam, I., Jha, H., Liu, N. & Schmuki, P. A review of photocatalysis using self-organized TiO_2 nanotubes and other rrdered oxide nanostructures. *Small* **8**, 3073–3103 (2012).
25. Ye, M. D., Gong, J. J., Lai, Y. K., Lin, C. J. & Lin, Z. Q. High-efficiency photoelectrocatalytic hydrogen generation enabled by palladium quantum dots-sensitized TiO_2 nanotube arrays. *J. Am. Chem. Soc.* **134**, 15720–15723 (2012).
26. Huo, K. F., Wang, H. R., Zhang, X. M., Cao, Y. & Chu, P. K. Heterostructured TiO_2 nanoparticles/nanotube arrays: in situ formation from Amorphous TiO_2 nanotube arrays in water and enhanced photocatalytic activity. *ChemPlusChem* **77**, 323–329 (2012).
27. Lin, J. *et al.* A facile route to fabricate an anodic TiO_2 nanotube-nanoparticle hybrid structure for high efficiency dye-sensitized solar cells. *Nanoscale* **4**, 5148–5153 (2012).
28. Varghese, O. K., Gong, D. W., Paulose, M., Grimes, C. A. & Dickey, E. C. Crystallization and high-temperature structural stability of titanium oxide nanotube arrays. *J. Mater. Res.* **18**, 156–165 (2003).
29. Lai, Y. K. *et al.* Nitrogen-doped TiO_2 nanotube array films with enhanced photocatalytic activity under various light sources. *J. Hazard. Mater.* **184**, 855–863 (2010).
30. Tang, Y. X. *et al.* Hierarchical TiO_2 nanoflakes and nanoparticles hybrid structure for improved photocatalytic activity. *J. Phys. Chem. C* **116**, 2772–2780 (2012).
31. Kota, A. K., Li, Y. X., Mabry, J. M. & Tuteja, A. Hierarchically structured superoleophobic surfaces with ultralow contact angle hysteresis. *Adv. Mater.* **24**, 5838–5843 (2012).
32. Kwon, G. *et al.* On-demand separation of oil-water mixtures. *Adv. Mater.* **24**, 3666–3671 (2012).
33. Dorrer, C. & Rühe, J. Superaerophobicity: repellence of air bubbles from submerged, surface-engineered silicon substrates. *Langmuir* **28**, 14968–14973 (2012).
34. Jin, M. H. *et al.* Underwater oil capture by a three-dimensional network architectured organosilane surface. *Adv. Mater.* **23**, 2861–2864 (2011).
35. Cassie, A. B. D. & Baxter, S. Wettability of porous surfaces. *Trans. Faraday Soc.* **40**, 546–551 (1944).
36. Lai, Y. K. *et al.* Designing superhydrophobic porous nanostructures with tunable water adhesion. *Adv. Mater.* **21**, 3799–3803 (2009).
37. Xue, Z. X. *et al.* A novel superhydrophilic and underwater superoleophobic hydrogel-coated mesh for oil/water separation. *Adv. Mater.* **23**, 4270–4273 (2011).
38. Zhang, L. B., Zhang, Z. H. & Wang, P. Smart surfaces with switchable superoleophilicity and superoleophobicity in aqueous media: toward controllable oil/water separation. *NPG Asia Mat.* **4**, E8 (2012).
39. Zhang, L. B., Zhong, Y. J., Cha, D. & Wang, P. A self-cleaning underwater superoleophobic mesh for oil-water separation. *Sci. Rep.* **3**, 2326; doi:10.1038/srep02326 (2013).
40. Lai, Y. K. *et al.* Bioinspired patterning with extreme wettability contrast on TiO_2 nanotube array surface: a versatile platform for biomedical applications. *Small* **9**, 2945–2953 (2013).
41. Dong, J., Yao, Z. H., Yang, T. Z., Jiang, L. L. & Shen, C. M. Control of superhydrophilic and superhydrophobic grapheme interface. *Sci. Rep.* **3**, 1733; doi:10.1038/srep01733 (2013).
42. Limongi, T. *et al.* Nanostructured superhydrophobic substrates trigger the development of 3D neuronal networks. *Small* **9**, 402–412 (2013).

Acknowledgements

The authors thank the Alexander von Humboldt (AvH) Foundation of Germany, EU Microcare project (FP7-PEOPLE-2009-IRSES/247641), the Natural Science Foundation of Jiangsu Province of China (Grant No. BK20130313) and the Environment and Water Industry Programme Office under the National Research Foundation of Singapore (Grant No. MEWR651/06/160) for the financial support of this work. We also acknowledge support from the Priority Academic Program Development of Jiansu Higher Education Institutions (PAPD).

Author contributions

Y.K.L. and L.F.C. conceived and designed the study. Y.K.L. wrote the manuscript. Y.K.L. and Y.X.T. performed the experiments. J.Y.H. and F.P. helped to do the experiments. Z.C. and K.Q.Z. and H.F. gave scientific advice. All the authors contributed to discussion and reviewed the manuscript.

Additional information

Supplementary information accompanies this paper at http://www.nature.com/scientificreports

Competing financial interests: The authors declare no competing financial interests.

How to cite this article: Lai, Y.K. *et al.* Bioinspired TiO_2 Nanostructure Films with Special Wettability and Adhesion for Droplets Manipulation and Patterning. *Sci. Rep.* **3**, 3009; DOI:10.1038/srep03009 (2013).